Research article

Aerodynamic efficiency of flapping flight: analysis of a two-stroke model

Z. Jane Wang

Theoretical and Applied Mechanics, Cornell University, Ithaca, NY 14853, USA
e-mail: jane.wang@cornell.edu

Summary

To seek the simplest efficient flapping wing motions and understand their relation to steady flight, a two-stroke model in the quasi-steady limit was analyzed. It was found that a family of two-stroke flapping motions have aerodynamic efficiency close to, but slightly lower than, the optimal steady flight. These two-stroke motions share two common features: the downstroke is a gliding motion and the upstroke has an angle of attack close to the optimal of the steady flight of the same wing. With the reduced number of parameters, the aerodynamic cost function in the parameter space can be visualized. This was examined for wings of different lift and drag characteristics at Reynolds numbers between 10^2 and 10^6. The iso-surfaces of the cost function have a tube-like structure, implying that the solution is insensitive to a specific direction in the parameter space. Related questions in insect flight that motivated this work are discussed.

Key words: efficiency, aerodynamics, flapping wing, flight.

Introduction

Quantitative studies have made much progress in revealing various aerodynamic mechanisms for force generation in flapping flight, as extensively reviewed (Weis-Fogh and Jensen, 1956; Ellington, 1984; Dickinson, 1996; Sane, 2003; Lehmann, 2004; Wang, 2005). Less clear is the relative cost of various wing motions that are capable of generating the same averaged force. For example, for a given wing, how does the aerodynamic cost of flapping flight compare to that of a fixed wing flight? A necessary first step in addressing the question of relative efficiency is to define a fair and relevant measure for cross-comparing different wing motions. With the model of aerodynamic forces and actuators, we can, in principle, determine efficient wing motions either in real animals or model systems. Suppose we succeed in doing so, the solutions may still be non-intuitive due to the fact that a typical wing motion is described by a large number of parameters. Moreover, some features in the predicted motions are specific to the model rather than the original system. The main purpose of this paper is to seek some common features of efficient flapping motions in a minimal model, as a step toward understanding the more complex ones.

Hovering, as opposed to forward flight, is a natural candidate for comparing the efficiency of two flight strategies: flapping *vs* steady flight. In hovering, a moving wing alone generates the required thrust without the need for additional propulsions. Here, the word efficiency is used to mean the inverse of the dimensionless cost. First, an energetic criterion is defined, with which the relative aerodynamic cost of employing different wing motions can be compared. Finding efficient wing motions requires an effective method for reducing the parameter space without excluding all of the efficient motions. One approach is to use the observed insect wing motions as a guide to construct families of wing motions described by a set of physical parameters. The idea

is that the odds of finding efficient solutions among insects' or birds' wing motions are likely to be higher than our random guesses. In the reduced parameter space, we can identify with energy-minimizing flapping wing kinematics for various insects, compare with observed motions, and recognize common features (Berman and Wang, 2007). In this paper, we seek the simplest efficient flapping wing motions that can be analyzed in detail. To this end, we consider a family of up and down motions described by six parameters and calculate the aerodynamic power in quasisteady limit. The parameter space was further reduced to four-dimensions, based on the reasoning described below. An advantage of working with the remaining four-parameter space is that it is possible to visualize the parameter space. The sensitivity of the cost function can be viewed with respect to the wing motion parameters, and in relation to classical steady wing motion.

A criterion for comparing the aerodynamic cost of a wing undergoing different hovering wing motions

For animals and airplanes, the total energetic cost is measured by the consumption of their respective fuels. At the limit where the conversion rate from chemical to mechanical energy is independent of the wing motion, the total cost is directly proportional to the mechanical work. The mechanical work done by a flapping wing includes aerodynamic and inertial components. The former is the work done to overcome fluid drag and the latter, work done to accelerate and decelerate the wing in a vacuum. The inertial cost can be calculated directly from the wing kinematics, and unless the elastic storage of the muscles is perfect, the net inertial cost is non-zero. The aerodynamic cost can be measured experimentally, calculated using direct numerical simulations, or estimated by quasi-steady force models.

The aerodynamic efficiency of transport of a classical airfoil in steady forward flight is determined by the lift:drag ratio, which is

the inverse of the aerodynamic work required to transport a unit weight over a unit distance. A similar ratio can be defined for the efficiency of endurance, which is proportional to the inverse of the aerodynamic power required to support a unit weight. These ratios are often used to compare the relative efficiency of different airfoils: the higher the ratio, the more efficient the airfoil. For flapping motions, in addition to cross-comparing different wing shapes, it is of interest to investigate the relative efficiency of the same airfoil undergoing different wing motions, which is the focus of this work.

In the case of a hovering insect, the wing and the weight are given, and we seek the wing motion that minimizes the mechanic power subject to the constraint of the weight balance. Specifically, the aerodynamic cost of endurance ($P*$) is defined as the dimensionless aerodynamic power to support a unit weight:

$$P* = \frac{\int_0^T [\vec{F}(t)\cdot\vec{U}(t) + \vec{\tau}(t)\cdot\vec{\Omega}(t)]\mathrm{d}t}{MgTU_{\mathrm{ref}}}, \quad (1)$$

with the constraint:

$$\frac{1}{T}\int_0^T \vec{F}(t)\cdot\hat{z}\mathrm{d}t = Mg , \quad (2)$$

where $\vec{F}(t)$ and $\vec{U}(t)$ are instantaneous aerodynamic force and wing translational velocity, $\vec{\tau}(t)$ and $\vec{\Omega}(t)$ the instantaneous aerodynamic torque and wing angular velocity, Mg the weight, and T the period. $P*$ is dimensionless, and the reference velocity $U_{\mathrm{ref}}=\sqrt{2Mg/\rho A}$ is constant for a specific wing of area A and weight Mg. The inertial cost can be added if we have a model of elastic storage of the muscles (Berman and Wang, 2007). For the piece-wise constant motions studied here, the inertial cost is zero except near the transition.

Note that in the case of steady wing motion (Fig. 1B), $P*$ has the familiar form: $P*=C_D(\alpha)/C_L^{3/2}(\alpha)$, where $C_L(\alpha)$ and $C_D(\alpha)$ are lift and drag coefficients, respectively. For general wing motions, this simple ratio no longer holds, and thus maximizing the averaged lift:drag ratio is not equivalent to minimizing the aerodynamic power. We further note that $P*$ is proportional to the specific power, power per mass supported (Ellington, 1984). The main difference is that here the specific power is only compared among the motions that generate the same force. This difference matters when the aerodynamics force coefficients depend indirectly on the net force due to, for example, the change of the Reynolds number of the flow required to generate the specified force.

Two-stroke wing motions and a model of quasi-steady forces
The steady forward flight motion is defined by the wing velocity, U, and the angle of attack, α (stroke-I, Fig. 1A). Similarly, the rotary wing motion is defined by the angular velocity, Ω and α. The simplest flapping motion is a back-and-forth motion, which can be viewed as a rotary motion projected onto the diameter keeping the same angle of attack and velocity (Fig. 1B). In the quasi-steady limit considered here, these symmetrical back and forth motions are equivalent to the rotary motion. Among them, the one that minimizes $P*$ has α_m that minimizes $C_D/C_L^{3/2}$ and U_m that balances the weight at $\alpha_m=\frac{1}{2}\rho C_L(\alpha_m)U_m^2 A=Mg$.

The next simplest flapping motion (Stroke-II, Fig. 1E) consists of two constant motions arranged in a V-shape, and is defined by seven parameters: the velocity ($U_{d,u}$), the angle of attack ($\alpha_{d,u}$), the
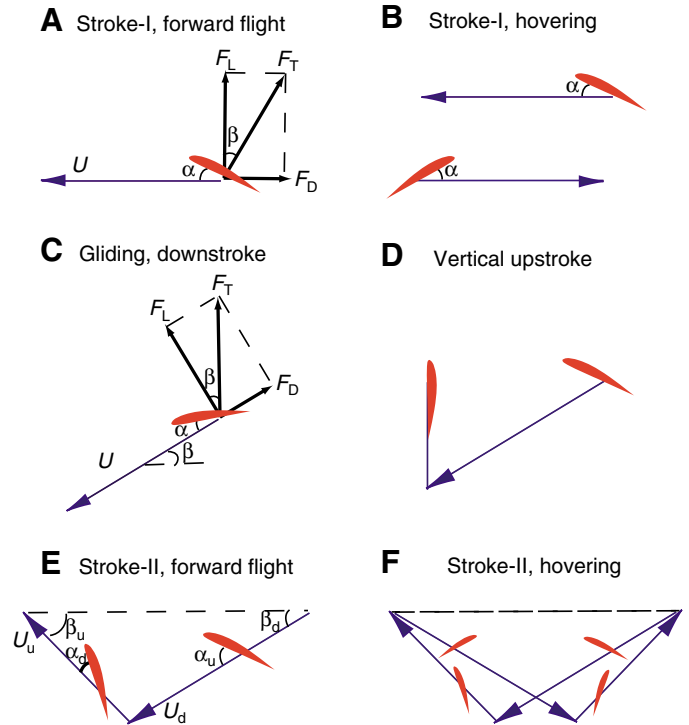

Fig. 1. Wing motions. (A) Steady forward flight, (B) hovering using a pair of motion in part a, (C) gliding (rotation of A), (D) gliding followed by a vertical upstroke, (E) gliding followed by a lift-generating upstroke, and (F) hovering using a mirror pair of E. Parameters: $\alpha_{d,u}$ are the angle of attack in down- and upstrokes, respectively, $\beta_{d,u}$ the angle of the stroke plane, $U_{d,u}$ the velocity, and ϵ the fraction of time spent on the upstroke, i.e. $U_u/U_d=[(1-\epsilon)/\epsilon]/(\sin\beta_d/\sin\beta_u)$.

angle of stroke path ($\beta_{d,u}$) during down (d) and up (u) strokes, and the fraction of a period spent on the upstroke (ϵ). Six of them are independent if we further require that two ends of V maintain the same altitude. A pair of mirror images of each V-shape forms a figure-eight (Fig. 1F), which is a hovering motion.

These two-stroke motions are piece-wise constant, thus the main unsteady aerodynamic effect is the dynamic stall, during which the leading edge vortex forms and remains attached while producing a force that is roughly constant at a given angle (Francis and Cohen, 1933; Ellington, 1984; Dickinson and Götz, 1993; Ellington et al., 1996; Wang, 2000; Usherwood and Ellington, 2002). At this limit, the empirical formula to fit the lift-drag at relative low Reynolds numbers ($\sim10^2$) can be expressed as (Wang, 2005):

$$C_L(\alpha) = C_L (\pi/4) \sin2(\alpha-\alpha_{0l}) , \quad (3)$$

$$C_D(\alpha) = C_D(0) + \tfrac{1}{2}[C_D(\pi/2)-C_D(0)] [1-\cos2(\alpha-\alpha_{0d})] , \quad (4)$$

where C_L and C_D are lift and drag coefficients, respectively, α the angle of attack, α_{0l} the angle at which lift is zero and α_{0d} the angle at which the drag is minimal. α_{0l} and α_{0d} are non-zero for asymmetrical airfoils. Similar form was also obtained to fit the experimental measurements of lift–drag characteristics of helicopter blades during dynamic stall at much higher Reynolds numbers of about 10^6 (Leishman, 2000). The fit of this formula to airfoil data is shown in Fig. 2. Note that Eqn 3 differs from the classical Joukowski's lift in its angle dependence, $\sin2\alpha$ rather than $\sin\alpha$, and it is to be applied to all angles of attack during dynamic stall.
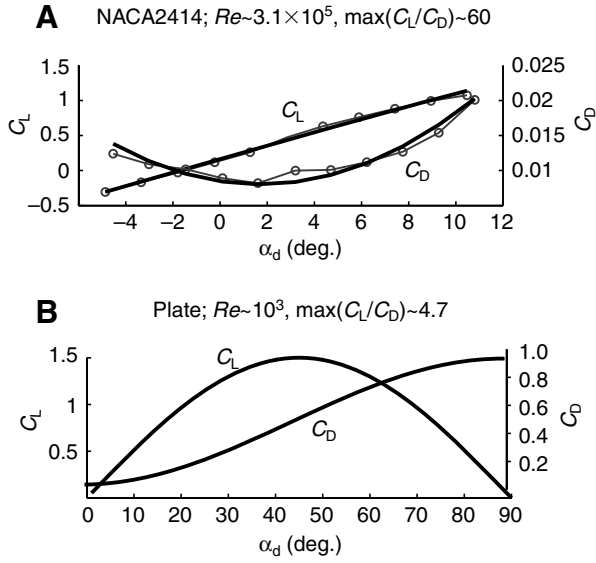
A   NACA2414; Re~3.1×10⁵, max(C_L/C_D)~60

B   Plate; Re~10³, max(C_L/C_D)~4.7

Fig. 2. Lift and drag coefficients. (A) An airfoil (NACA2414) at Re~3×10⁵. Circles are experimental data (Selig, 2002) and solid lines are given by C_L=2.77sin2(α+0.03), C_D=0.0086+0.24[1−cos2(α−0.02)]. (B) A low Reynolds number plate at Re~10³, C_L=1.5sin2α, C_D=1.1−cos2α.

Efficient two-stroke wing motions

In this minimal model, the parameter space is six-dimensional, which is still difficult to visualize directly. To further reduce the number of parameters, we make two observations. The first is that the classical airfoil motion of a fixed or rotating wing uses only aerodynamic lift, but not drag, to support a weight (Wang, 2004). If the airfoil is reoriented such that the net force is vertical (Fig. 1C), as in gliding, the wing can support an additional weight by a factor of $\sqrt{1+[C_D^2(\alpha)/C_L^2(\alpha)]}-1$. Consider the ideal case in which the downstroke is a gliding motion and the upstroke returns instantaneously, consuming no energy, to support a specified weight, U_I/U_d=$[1+C_D^2(\alpha)/C_L^2(\alpha)]^{\frac{1}{4}}$ and P_{II}^*/P_I^*=$[1+C_D^2(\alpha)/C_L^2(\alpha)]^{\frac{3}{4}}<1$. This gliding motion is more efficient and is used as the downstroke of the flapping motions studied below.

An upstroke must return in a finite time and it costs energy. At first sight, the least costly upstroke seems to be the vertical upstroke at zero angle of attack (Fig. 1D), because it moves along the shortest path and the wing experiences the least drag. However, this is not the case (Fig. 3). To find a more efficient upstroke, we note the angle dependence of the aerodynamic force at small angles. As α deviates from zero, to the leading order, the lift increases as α, as given by the Kutta–Joukowski theory, while the drag increases as α^2. At small α, $\alpha^2 \ll \alpha$, thus an upstroke at small angle of attack generates a lift at a relatively small cost, which can be advantageous compared to that with α=0, which generates no lift. These lift-generating strokes replace the vertical upstroke. The two-stroke motion is now described by four parameters, (α_u, β_u, ϵ, α_d), and the corresponding P^* is given by:

$$P^* = \frac{\frac{1}{2}\rho A[C_D(\alpha_d)U_d^3 T_d + C_D(\alpha)U_u^3 T_u]}{MgTU_{ref}}, \qquad (5)$$

where

$$U_d = \frac{\sqrt{\frac{2Mg}{\rho A}}}{\sqrt{C_T(\alpha_d)(1-\epsilon) + \left(\frac{1-\epsilon}{\epsilon}\frac{\sin\beta_d}{\sin\beta_u}\right)^2 [C_L(\alpha_u)\cos\beta_u - C_D(\alpha_d)\sin\beta_u\epsilon]}}, \qquad (6)$$

$$\frac{U_u}{U_d} = \frac{1-\epsilon}{\epsilon}\frac{\sin\beta_d}{\sin\beta_u}, \qquad (7)$$

$$C_T = \sqrt{C_L^2 + C_D^2}. \qquad (8)$$

We minimize P^* with respect to (ϵ, β_u, α_u) for each downstroke parameterized by α_d in Matlab.

The cost to transit between the two piece-wise constant strokes is neglected in the calculation of P^*. Its contribution is small compared to the rest of the stroke in the large stroke-amplitude limit. More interestingly, the wing pitch reversal does not necessarily require additional power (Bergou et al., 2007; Berman and Wang, 2007), which is discussed later.
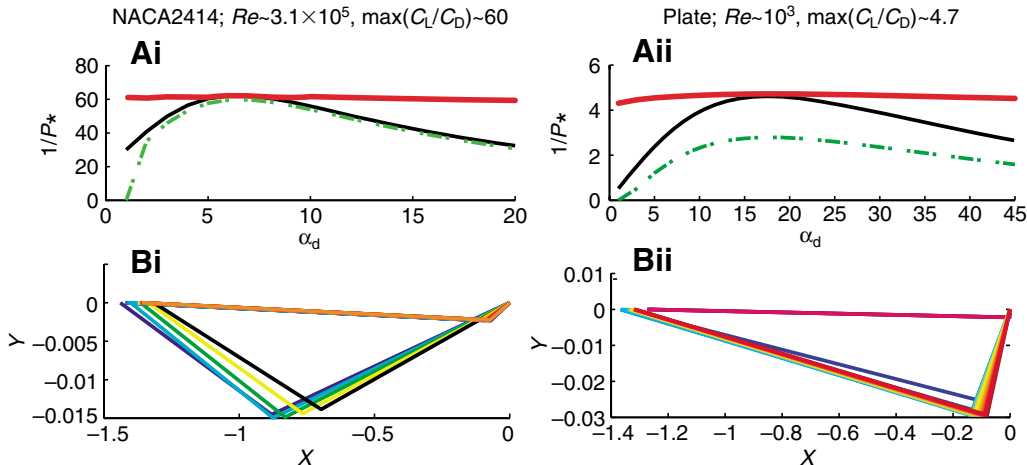
NACA2414; Re~3.1×10⁵, max(C_L/C_D)~60   Plate; Re~10³, max(C_L/C_D)~4.7

Fig. 3. Two-stroke flapping motions near the optimum. (A) 1/P^* vs α_d for steady motion (black), two-stroke motion composed of a gliding downstroke followed by a vertical upstroke (green), and two-stroke motion composed of the same gliding stroke followed by a near optimal lift-generating upstroke (red). (B) The near optimal down- and upstrokes. Ai, Bi, airfoil NACA2414 at Re~3×10⁵; Aii, Bii, plate at Re~10³.
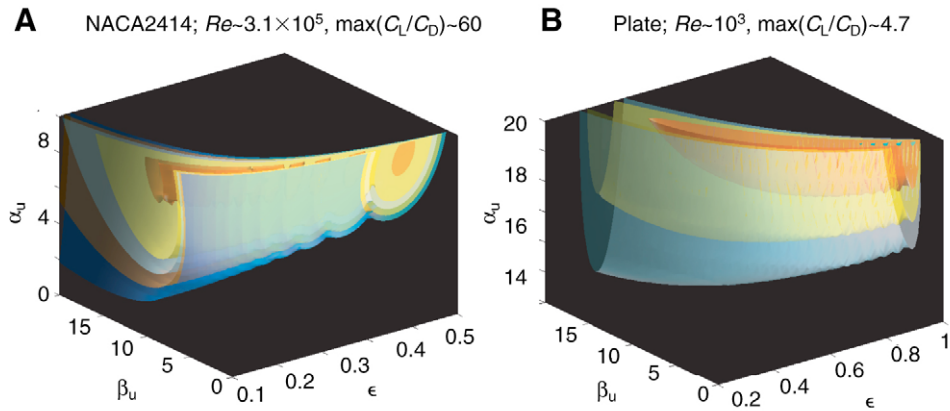
A   NACA2414; Re~3.1×10^5, max(C_L/C_D)~60   **B**   Plate; Re~10^3, max(C_L/C_D)~4.7

Fig. 4. The isosurface of $1/P^*$ as a function of α_d, β_u, ϵ. It has a cylindrical-like shape whose longitudinal direction corresponds to the multiple solutions shown in Fig. 3. Starting from the innermost surface, the iso-surface values are $1/P^*$=58.5, 58, 57.5, 57 (A) and 4.7, 4.6, 4.5, 4.4 (B).

Fig. 3A compares $1/P^*$ among three kinds of wing motions: back-and-forth motion with a constant angle of attack (α_d) two-stroke, composed of a gliding downstroke with the same angle of attack (α_d) followed by a vertical upstroke at zero angle of attack, and two-stroke composed of the same gliding stroke followed by an optimized upstroke. Two representative Reynolds numbers (Re) are shown: 10^3, close to that of an insect, and 3×10^5, close to that of a low-speed airplane. The maximum lift:drag ratios are 4.7 and 60, respectively. In both cases, there are multiple asymmetrical down-and-up flapping motions (Fig. 3B), whose P^* are close to minimal, but slightly higher than the minimum of $C_D/C_L^{3/2}$ of the steady wing motion.

By definition, the first derivative of a function at minimum (inside the domain) is zero, and the sensitivity to parameters is given by higher order derivatives. In the case of back-and-forth motions, the efficiency drops relatively quickly as the angle of attack deviates from the optimal angle, whereas in the case of up-and-down motions, the minimum is much more flat. Fig. 4C shows the iso-surfaces of $1/P^*$ as a function of parameters of the upstroke, (ϵ, α_u, β_u) for a given α_d. Their shapes near the maximum have a tube-like structure. The longitudinal direction of the tube corresponds to the multiple solutions found here.

Among the parameters in the quasi-steady force model, the one that is most sensitive to Re is $C_D(0)$; $C_D(0)$~$1/\sqrt{Re}$. To investigate

the effect of Re, $C_D(0)$ is varied from 0.3 to 0.003, which corresponds to Re from ~10^2 to ~10^6, estimated using the Blasius theory of flow past a plate (Glauert, 1947). To see the effect of wing shape, the calculation was repeated using ten randomly chosen published lift–drag characteristics for airfoils in NACA-4digit, DH and Xfoil-series (Selig, 2002). For low Reynolds number plates, $C_L(\pi/4)$ and $C_D(\pi/2)$ are varied between 1 and 2.5, to simulate the effect of the sharpness of the wing tip (Wang, 2000). The extended tube structure is found for all tested Reynolds numbers and wing shapes.

Concluding remarks

The above analysis was partly motivated by the question concerning the relative efficiency of flapping and steady wing motions that support the same weight. The two-stroke model suggests that at the limit where the lift and drag are described by the translational quasi-steady forces, the most efficient motion to support a given weight is the steady wing motion at the optimal angle of attack. There are multiple flapping motions that are very close to the optimum. The efficient two-stroke motions have in common that the downstroke is a gliding motion at an arbitrary angle of attack and the upstroke operates near the optimal angle of attack. We are currently investigating if flapping flight can be more efficient than the steady wing motion when the unsteady aerodynamics effects are included.

Another motivation came from our interest in understanding whether insects are aerodynamically efficient; specifically, whether hovering insects have found some energy-minimizing wing kinematics, given that hovering is an energy-demanding mode of flight. The idea of optimization in biological systems is open to debate. Without testable predictions, however, it is difficult to make progress. Using the same criterion as discussed here, various published wing strokes were examined (Berman and Wang, 2007), for fruit flies (Ennos, 1989; Fry et al., 2003), a bumblebee (Dudley and Ellington, 1990) and a hawkmoth (Willmott and Ellington, 1997), and it was found that some of the specific features of the predicted energy-minimizing hovering kinematics, e.g. the frequency and the wing stroke pattern, are qualitatively and quantitatively similar to the previously observed data. This, however, does not imply that all hovering insects fly using a single pattern of wing motion. Optimal wing motion depends on the wing morphology and lift–drag characteristics. Even for a specific wing, there can be many solutions that are very close to optimal, as indicated here with a four-parameter model. This multiplicity of
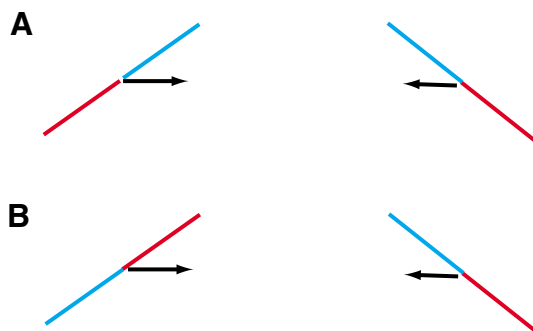

Fig. 5. Strokes A and B generate almost the same amount of force. The only difference occurs near the end of the stroke when the wing reverses its pitch. In A the leading edge remains the same, and in B it switches. The wing pitching in stroke A can be facilitated by wing inertia and aerodynamic torque as the wing decelerates (Berman and Wang, 2007; Bergou et al., 2007).

solutions does not contradict the idea that energy-minimizing shapes the wing kinematics. Instead, we should expect variations in the observed wing kinematics that have comparable efficiency near the optimal.

Finally, to comment on the transition between the up- and downstrokes, the cost of which is assumed to be small. Although muscles in insects are known to be capable of actively pitching the wing (Ellington, 1984; Dickinson et al., 1993), the net power required to pitch the wing in the observed motions of a dragonfly, a fruit fly and a hawkmoth was found to be negative (Bergou et al., 2007). Thus in theory, wing pitching can be aided by aerodynamic torque and does not require additional power. This, and the fact that almost all insects maintain the same leading edge (Fig. 5), suggest that insects may benefit from passive wing pitch reversal during steady flight to simplify control.

References

Bergou, A., Xu, S. and Wang, Z. J. (2007). Passive wing pitch reversal in insect flight. *J. Fluid Mech.* **591**, 321-337.

Berman, G. and Wang, Z. J. (2007). Energy minimizing kinematics in hovering insect flight. *J. Fluid Mech.* **582**, 153-168.

Dickinson, M. H. (1996). Unsteady mechanisms of force generation in aquatic and aerial locomotion. *Am. Zool.* **36**, 537-554.

Dickinson, M. H. and Götz, K. G. (1993). Unsteady aerodynamic performance of model wings at low Reynolds numbers. *J. Exp. Biol.* **174**, 45-64.

Dickinson, M. H., Lehmann, F. O. and Götz, K. G. (1993). The active control of wing rotation by Drosophila. *J. Exp. Biol.* **182**, 173-189.

Dudley, R. and Ellington, C. P. (1990). Mechanics of forward flight in bumblebees. II. Quasi-steady lift and power requirements. *J. Exp. Biol.* **148**, 53.

Ellington, C. P. (1984). The aerodynamics of hovering insect flight. I–V. *Philos. Trans. R. Soc. Lond. B Biol. Sci.* **305**, 1-181.

Ellington, C. P., van den Berg, C., Willmott, A. P. and Thomas, A. L. R. (1996). Leading-edge vortices in insect flight. *Nature* **384**, 626-630.

Ennos, A. R. (1989). The kinematics and aerodynamics of the free flight of some diptera. *J. Exp. Biol.* **142**, 49-85.

Francis, R. H. and Cohen, J. (1933). The flow near a wing which starts suddenly from rest and then stalls. *Aero. Res. Counc. Rep. Memo.* **1561**, 90.

Fry, S. N., Sayaman, R. and Dickinson, M. H. (2003). The aerodynamics of free-flight manuevers in Drosophila. *Science* **300**, 495-498.

Glauert, H. (1947). *The Elements of Aerofoil and Airscrew Theory.* Cambridge: Cambridge University Press.

Lehmann, F. O. (2004). The mechanisms of lift enhancement in insect flight. *Naturwissenschaften* **91**, 101-122.

Leishman, J. (2000). *Principles of Helicopter Aerodynamics.* Cambridge: University of Cambridge.

Sane, S. (2003). The aerodynamics of insect flight. *J. Exp. Biol.* **206**, 4191-4208.

Selig, M. (2002). Online database for airfoil lift-drag characteristics. http://www.aae.uiuc.edu/m-selig/pub/lsat/vol1-3.

Usherwood, J. R. and Ellington, C. P. (2002). The aerodynamics of revolving wings. II. Propeller force coefficients from mayfly to quail. *J. Exp. Biol.* **205**, 1565-1576.

Wang, Z. J. (2000). Vortex shedding and frequency selection in flapping flight. *J. Fluid Mech.* **410**, 323-341.

Wang, Z. J. (2004). The role of drag in insect hovering. *J. Exp. Biol.* **207**, 4147-4155.

Wang, Z. J. (2005). Dissecting insect flight. *Annu. Rev. Fluid Mech.* **37**, 183-210.

Weis-Fogh, T. and Jensen, M. (1956). Biology and physics of locust flight. I. Basic principles in insect flight. A critical review. *Proc. R. Soc. Lond. B Biol. Sci.* **239**, 239, 415-458.

Willmott, A. P. and Ellington, C. P. (1997). The mechanics of flight in the hawkmoth *Manduca sexta.* I. Kinematics of hovering and forward flight. *J. Exp Biol.* **200**, 2705-2722.